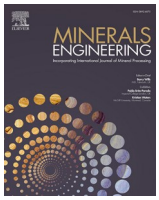
Minerals Engineering 205 (2024) 108479



Contents lists available at ScienceDirect

Minerals Engineering

journal homepage: www.elsevier.com/locate/mineng





An improved model for predicting froth recovery

S.J. Neethling *, D. Mesa, P.R. Brito-Parada

Imperial College London, United Kingdom

ARTICLE INFO

Keywords:
Froth Flotation
Froth recovery
Modelling
Froth stability
Bubble loading

ABSTRACT

In froth flotation, froth recovery is a key factor as it quantifies the effect that the froth has on the overall cell recovery. Froth recovery is affected by a number of variables, including froth stability, particle size and density, and the operating conditions of the flotation cell. Despite its importance, modelling froth recovery is challenging due to the large number of competing effects involved. In this paper, we present a model for froth recovery that takes into account the effects of detachment and subsequent transport of particles. The model is phenomenological and is derived from a set of coupled partial differential equations used to describe both liquid and particle motion within a froth. An analytical algebraic solution is obtained for the froth recovery by making a number of assumptions, which are discussed and justified in the paper. This model is related to a previous model produced by the authors, in which froth recovery was described in terms of a constant particle detachment fraction. Conversely, this enhanced model includes an improved description for particle detachment behaviour during coalescence events, allowing for a variable particle detachment fraction. The key parameters in the model are two dimensionless groups. The first group combines the particle settling velocity, the air addition rate and froth stability parameters such as air recovery and the change in bubble size over the froth, while the second key dimensionless group is the ratio of the surface loading on the incoming bubbles to the maximum surface loading. This model is compared to experimental results and is shown to accurately describe the evolution of the froth recovery behaviour down a bank of cells in response to the decreasing froth stability.

1. Introduction

Froth recovery is an important factor in flotation performance as it quantifies the effect that the froth has on the overall recovery from a flotation cell. Froth recovery is strongly affected by both froth stability and particle properties such as size and density (Rahman et al. (2012); Yianatos et al. (2008)). Both of these effects will be considered in the modelling presented in this paper.

Froth recovery is usually defined as the proportion of particles that enter the froth attached to bubbles that pass into the concentrate (Finch and Dobby (1990)). It is important to note that this is not the same as the proportion of particles that remain attached within the froth. This is because the net motion of liquid within a typical flotation froth is upwards and liquid will therefore carry some of the detached particles into the concentrate. A previous study (Hadler, 2015) using measurements of both bubble loading and concentrate flows indicates that the majority of particles that enter the froth attached and that make it into the concentrate do so as unattached particles. This transport of detached particles is the main reason why froth recovery is particle size and density dependent.

It is this interconnected dependence on both detachment and subsequent transport that makes froth recovery challenging to model. In previous papers the authors have developed Computational Fluid Dynamics (CFD) like models for flotation froths (Neethling et al. (2000); Neethling et al. (2005); Neethling and Cilliers (2002b); Neethling and Cilliers (2002a); Neethling and Cilliers (2003)) that involve solving Partial Differential Equations (PDEs), but which allows the performance of flotation froths, including the froth recovery, to be predicted. While there are no analytical solutions for the full set of PDEs as a number of them are highly non-linear, it is possible to make assumption that allow analytical expressions to be developed. In previous work the authors have developed such expressions for the water recovery (Neethling et al. (2003)), entrainment factor (Neethling and Cilliers (2009)) and, crucially in the context of this paper, froth recovery (Neethling, 2008).

As mentioned above, during the coalescence of bubbles within the froth some particles that are attached to the lost surface area will become detached and free to move. Crucially, though, some particles will remain attached, resulting in an increase in the mass loading per

* Corresponding author at: Imperial College, South Kensington Campus, London SW7 2AZ, UK.
E-mail address: s.neethling@imperial.ac.uk (S.J. Neethling).

https://doi.org/10.1016/j.mineng.2023.108479
Received 25 July 2023; Received in revised form 17 October 2023; Accepted 22 October 2023
Available online 6 November 2023
0892-6875/© 2023 The Authors. Published by Elsevier Ltd. This is an open access article under the CC BY license (http://creativecommons.org/licenses/by/4.0/).

bubble surface area (but a decrease per froth volume) as the bubbles rise and coalesce within the froth. In the earlier paper on froth recovery (Neethling, 2008) it was assumed that this detaching fraction remained constant. The experimental data accompanying the paper suggested that this was not actually the case, with the calculated detachment fraction varying with operating conditions and position in the circuit. It is also logical that this fraction should change, especially with bubble loading, as a constant detachment fraction means that there is no limit to the increase in the loading as bubble size increases, whereas in reality there is a physical limit to the mass of particles that can be accommodated on a given film area.

In this paper we will therefore be relaxing this assumption and thereby developing an improved model for froth recovery. In addition, we will be examining the limits on model validity, together with relationships for the froth recovery where these limits are exceeded.

2. Constant detachment fraction

The starting point for all the modelling described in this paper is the relationship between the change in mass loading per bubble surface area, L, and the specific surface area of the bubbles, S_b. This first differential equation is:

$$\frac{dL}{dS_b} = -\frac{L}{S_b}(1-f) \tag{1}$$

Before developing the model for the variable detachment fraction it is useful to re-examine the modelling and modelling assumptions for the case where the detachment fraction, f, is constant (a more detailed derivation can be found in (Neethling, 2008)). Integrating equation (1) for a constant f, the change in loading can be written as a function of the change in the specific surface area:

$$\frac{L_2}{L_1} = \left(\frac{S_{b1}}{S_{b2}}\right)^{1-f} \tag{2}$$

As the specific surface area of the bubbles is inversely proportional to the equivalent bubble radius, the change in loading can be written as a function of the change in bubble radius, r:

$$\frac{L_2}{L_1} = \left(\frac{r_2}{r_1}\right)^{1-f} \tag{3}$$

The next key aspect of the modelling is to predict what will happen to the particles after they become detached. This will strongly depend on their settling velocity, v_{set}, and the motion of the liquid. The average motion of the liquid in the froth is upwards and, if we assume that the cell has vertical walls, the average vertical flux will be constant below the level of the overflow. On the other hand, the bubbles will grow in size with height in the froth due to coalescence. The liquid content is a strong function of bubble size, with larger bubbles resulting in lower liquid contents. This means that, given a constant liquid flux and decreasing liquid content, the vertical liquid velocity will increase with height in the froth.

It is possible to calculate the liquid content of the froth as a function of the bubble size at the location, r, the superficial gas velocity, v_g, the air recovery, α, and the overflowing bubble size, r_{out}, by making the assumption that we are above the capillary boundary layer and that the dominant forces for liquid drainage are gravity and viscous dissipation. We can therefore calculate the bubble size, r_{crit}, at the critical height in the froth where the downward particle setting velocity equals the upward velocity of the liquid (see (Neethling, 2008) for derivation):

$$\text{if } \alpha < \frac{1}{2}: \; r_{crit} = \sqrt{\frac{v_{set}}{v_g \alpha(1-\alpha)}}\, r_{out} \tag{4}$$

$$\text{if } \alpha \geq \frac{1}{2}: \; r_{crit} = \sqrt{\frac{4v_{set}}{v_g}}\, r_{out} \tag{5}$$

Note that this critical bubble size does not depend on the form of the relationship between bubble size and height in the froth. This relationship is also independent of the assumption that the detachment fraction is constant, and therefore can be used in all the subsequent modelling. However, as this equation assumes that the walls are vertical, the resulting model cannot be directly used for crowded cells. Further work is required to develop and validate a similar model with a relaxed assumption on the wall's geometry, as there is a clear gap in experimental data on the effect of crowders on froth recovery. Furthermore, this model also assumes that there is no wash water addition. While the underlying modelling used to produce this relationship can be adapted for cells with wash water, the concept of the critical bubble size may lose validity in such scenarios. This is because wash water is often added at a rate higher than the concentrate rate, leading to a net downward flow of water within the cell. Consequently, in that scenario there would be no specific point at which the settling velocity and liquid velocity exactly cancel one another out.

The motion of the particles in the froth is the result of three effects, namely particle settling, liquid motion and dispersion, with vertical dispersion being caused by the fact that there is a distribution of vertical liquid velocities around the mean velocity. In order to use the critical bubble size relationship, we need to make a further assumption, namely that dispersion of the particles can be neglected, with settling and liquid motion being the dominant effects. Because the concentration of previously attached particles will increase with height in the froth, the dispersion of these particles would be downwards. This means that assuming dispersion is negligible will result in a slight over-estimation of the froth recovery.

If we are assuming that dispersion is negligible, then particles will move upwards in the froth if the settling velocity is lower than the upward liquid velocity and vice versa. Since the upward liquid velocity increases with height, this means that particles released in a region where the settling velocity is lower than liquid velocity will move upwards to where the liquid velocity is even higher and therefore continue to move upwards until they are recovered to the concentrate, whereas particles released where the settling velocity is higher than the upward liquid velocity will move downwards into regions where the liquid velocity is even lower and will therefore ultimately fall out of the froth.

This means that particles that are still attached at the critical height/bubble size where the liquid velocity equals the settling velocity will be recovered even if they subsequently detach, whereas particles released below this point will fall out of the froth. This means that the froth recovery, R_f, can be written in terms of this critical bubble size and the loading at this critical location:

$$R_f \approx \frac{Q_{air} L_{crit} S_{bcrit}}{Q_{air} L_{in} S_{bin}} = \frac{L_{crit} r_{in}}{L_{in} r_{crit}} \tag{6}$$

Note that this relationship is also independent of the assumption that the detachment fraction is constant. If we now make the assumption that the detachment fraction, f, is constant and that equation (3) therefore applies and further combine this with equations (4) and (5), we arrive at the following relationship for the froth recovery:

$$R_f \approx {N_{Rf}}^f \tag{7}$$

$$\text{where} \quad \text{if } \alpha < \frac{1}{2}: N_{Rf} = \sqrt{\frac{v_g \alpha(1-\alpha)}{v_{set}}}\left(\frac{r_{in}}{r_{out}}\right) \tag{8}$$

$$\text{if } \alpha \geq \frac{1}{2}: \; N_{Rf} = \sqrt{\frac{v_g}{4v_{set}}}\left(\frac{r_{in}}{r_{out}}\right) \tag{9}$$

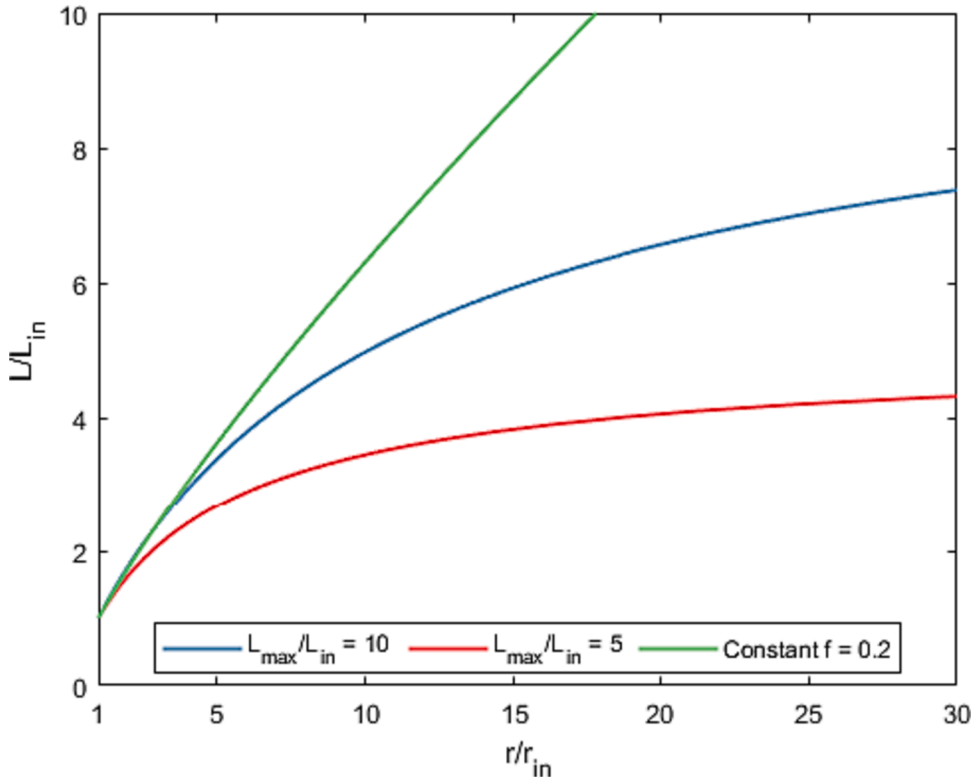


Fig. 1. Bubble loading as a function of bubble size, both relative to the incoming values. Predictions for linear change in detachment fraction with loading with two different maximum loading values and an $f_0 = 0.05$ compared to a constant detachment fraction with an $f = 0.2$.

Note that, unlike in the previous paper, the relationship has been written out in term of the dimensionless group, N_{Rf}, which incorporates the settling velocity and froth parameters. Because the settling velocity will be approximately proportional to the particle diameter squared, N_{Rf} will be approximately inversely proportional to the particle diameter, with a proportionality that is dependent on the froth parameters and, therefore, the operating conditions of the cell.

3. Variable detachment fraction

In the derivation above (and our previous paper), it was assumed that the fraction of material becoming detached during a coalescence event, f, was constant. In reality, f is likely to vary with loading, with more heavily loaded films having a higher proportion of their particles fall off than less highly loaded films. Ultimately the loading will approach a maximum loading for the film and at this point all the attached particle on the lost surface area must become detached during a coalescence event (i.e. f must equal 1 at some maximum loading). The exact form of this relationship is unknown and would be very difficult to find experimentally.

The derivation given in this paper could be readily repeated for any form of this relationship should the appropriate experiments be carried out to determine the form, but given the absence of such data, the simplest relationship that captures this behaviour will be used, namely a linear relationship between the detachment fraction, f, and the loading, L.

Linear change in f with a change in surface loading - In this section we will examine the effect of an f that varies linearly with loading. We will assume that there is an inherent fraction of material that falls off from even lightly loaded films, f_0. As the loading increases, the films will reach a point at which they are fully loaded and therefore cannot accommodate any more material during a coalescence event. This loading will be designated L_{max}, with a value of f at this point of 1:

$$f = f_0 + \frac{L}{L_{max}}(1 - f_0) \tag{10}$$

In order to ascertain how loading varies with specific surface area under this model, equation (10) will be used in conjunction with equation (1):

$$\frac{dL}{dS_b} = -\frac{L}{S_b}\left(1 - \left(f_0 + \frac{L}{L_{max}}(1 - f_0)\right)\right) \tag{11}$$

Integrating this equation between position 1 and 2 gives the following equation:

$$\frac{L_2}{L_1}\left(\frac{L_{max} - L_1}{L_{max} - L_2}\right) = \left(\frac{S_{b1}}{S_{b2}}\right)^{1-f_0} \tag{12}$$

If f_1 and f_2 are the values for f at loadings L_1 and L_2 respectively, then an equivalent expression to equation (12) is as follows:

$$\frac{L_2}{L_1} = \left(\frac{1 - f_2}{1 - f_1}\right)\left(\frac{r_2}{r_1}\right)^{1-f_0} \tag{13}$$

There is not a lot of data available on bubble loading changes as a function of the changes in bubble size and we will therefore be using the same data set as used in the previous analysis (Neethling, 2008). This data set is based on bubble loading measurements in the pulp using a froth viewer in which the mass of solids collected in the viewer chamber was measured and the loading calculated based on this mass together with the measured volume of air collected and bubble size distribution. Because the air displaces water, some of the collected solids will be lost, meaning that the measured loading is likely to be lower than the actual loading in the pulp, though hopefully with the correct trends. The surface loading was measured using touch samples obtained using the method outlined by (Sadr-Kazemi and Cilliers (2000); Ventura-Medina et al. (2004)). Because of film retraction, these surface loading measurements are likely to be slight over-estimates, but again with useful

trends. The surface bubble size was measured using image analysis based on the water-shedding algorithm (Sadr-Kazemi and Cilliers (1997)).

This data indicated that the f_0 values are quite small given that the implied average values for f trend towards a value of about 0.05 at low incoming loadings and the value of f_0 must be similar to and possibly slightly lower than this value. This implies that within a froth only a very small proportion of particles become detached during the coalescence of bubbles with low loadings. In the subsequent analysis we will use a value of 0.05 for f_0, though it will be demonstrated that as long as $f_0 \ll 1$, its exact value does not have a strong influence on the froth recovery calculated.

In Fig. 1 it can be seen that the loading behaves more realistically when using the variable detachment fraction as the bubble surface loading asymptotes towards a constant value rather than growing unbounded as it does with the constant detachment fraction.

4. Froth recovery with a variable detachment fraction

Froth recovery can also be estimated for a system in which f varies linearly with loading. By combining equations (4)–(6), (8)–(9), (12) and (13), the froth recovery can be obtained, where f_{crit} is the fraction of material becoming detached during coalescence at the position where the settling velocity equals the liquid velocity and f_{in} is the fraction becoming detached at the initial loading of the bubbles, both of which depend upon the loading at those points:

$$R_f = \frac{(1-f_{crit})}{(1-f_{in})} {N_{Rf}}^{f_0} \tag{14}$$

where

$$f_{in} = f_0 + \frac{L_{in}}{L_{max}}(1-f_0) \tag{15}$$

We can also write f_{crit} in a similar form, but this is not immediately useful as it requires that we know the loading at the critical height:

$$f_{crit} = f_0 + \frac{L_{crit}}{L_{max}}(1-f_0) \tag{16}$$

We can eliminate L_{max} by combining equations (15) and (16):

$$f_{crit} = f_0 + \frac{L_{crit}}{L_{in}}(f_{in}-f_0) \tag{17}$$

Combining with equation (13) we obtain an implicit equation for f_{crit}:

$$f_{crit} = f_0 + \left(\frac{1-f_{crit}}{1-f_{in}}\right)(f_{in}-f_0)\left(\frac{r_{crit}}{r_{in}}\right)^{1-f_0} \tag{18}$$

This can now be combined with equations (4) and (5) to eliminate r_{crit} and then using the definition in equations (8) and (9) and with a bit of rearranging this becomes:

$$f_{crit} = \frac{1 + f_0\left(\frac{1-f_{in}}{f_{in}-f_0}\right){N_{Rf}}^{1-f_0}}{1 + \left(\frac{1-f_{in}}{f_{in}-f_0}\right){N_{Rf}}^{1-f_0}} \tag{19}$$

This equation can now be used in conjunction with equations (14)–(15) in order to predict the froth recovery as they only depend upon inlet conditions and froth stability parameters.

Note that while this set of equations is slightly more complex than that for the constant f, once again the performance of the system can be characterised using a single dimensionless group, N_{Rf}, though this time together with the value for f_0 and the ratio of the incoming to maximum loading rather than a single average f value.

By combining equations (14), (15) and (19), an alternative form for the froth recovery can be obtained:

$$R_f = \frac{N_{Rf}}{\left(\frac{L_{in}}{L_{max}} + \left(1-\frac{L_{in}}{L_{max}}\right){N_{Rf}}^{1-f_0}\right)} \tag{20}$$

This equation is easier to implement than using equations (14) and (19), though less physically intuitive.

5. Validity ranges for the model and approximations for behaviour beyond these ranges

Because of the assumptions made in obtaining the model represented by equation (14) (together with equations (8)–(9), (15) and (19) or equation (20), there is a finite range of validity for these approximations. Also note that the range of validity discussed in this section is equally applicable to the model where f is assumed constant or any other model for f.

The main assumption that dictates the range of validity is that it is assumed that there is a location within the froth where the liquid velocity equals the settling velocity of the particles. This can be violated for very small particles and/or froths where the gas rate and stability are high. Under these circumstances the small particles can have a settling velocity that is lower than the upward liquid velocity at all locations in the froth. This is equivalent to $N_{Rf} > 1$. Under these circumstances the froth recovery should be 1 (or very close to 1 as dispersion could result in some particles falling out of the froth even if the average settling velocity is lower than the average liquid velocity at the bottom of the froth):

$$\text{if} \quad N_{Rf} > 1 : R_f \approx 1 \tag{21}$$

What happens at the other extreme of particles having a settling velocity greater than that of the liquid at all locations in the froth is slightly harder to assess. This is because, under these circumstances, particles that are released below the level of the overflow lip will fall out of the froth, but those particles released higher in the froth or released due to bursting at the froth surface could still be collected to the concentrate if they are released sufficiently close to the overflow that the horizontal transport is able to carry them over before they are able to settle downwards out of this region. Predicting this behaviour is more complex and would likely require the solution of the full set of PDEs for the liquid and particle motion. This limit would be reached when $r_{crit} = r_{lip}$. If we assume that $r_{lip} \approx r_{out}$, then this gives a minimum to the range of validity of $N_{Rf} = \frac{r_{in}}{r_{out}}$. This does not mean that the froth recovery will stop decreasing below this value, though the rate of decrease may not be as pronounced as the model presented in this paper predicts. There is an absolute minimum to which the froth recovery can drop and that is the froth recovery associated with only the particles attached to the films, with no contribution from unattached particles that entered the froth attached.

This minimum can be obtained by noting that under these circumstances:

$$R_{f,min} = \frac{Q_{air}L_{out}S_{bout}\alpha}{Q_{air}L_{in}S_{bin}} = \alpha\frac{L_{out}r_{in}}{L_{in}r_{out}} \tag{22}$$

Rearranging equation (12) over the full incoming to outflowing bubble size range gives us:

$$\frac{L_{out}}{L_{in}} = \frac{\frac{L_{max}}{L_{in}}}{\frac{L_{max}}{L_{in}} - 1 + \left(\frac{r_{out}}{r_{in}}\right)^{1-f_0}}\left(\frac{r_{out}}{r_{in}}\right)^{1-f_0} \tag{23}$$

Substituting equation (23) into (22) gives us the minimum possible froth recovery:

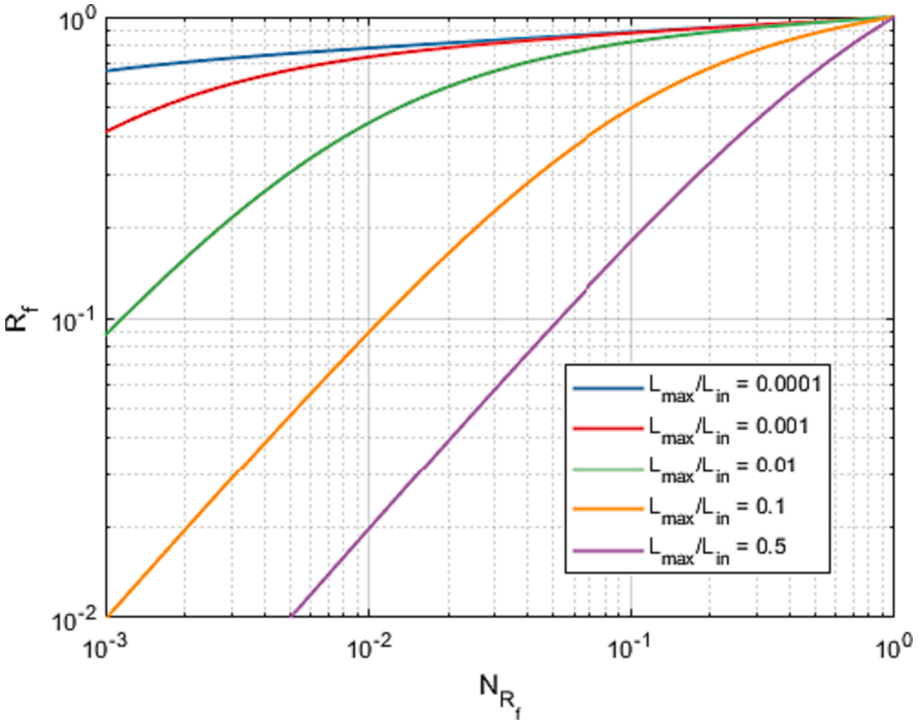


Fig. 2. Froth recovery as a function of N_{Rf} for different ratios of the initial to maximum bubble loading.

$$R_{f,min} = \alpha \frac{1}{1 - \frac{L_{in}}{L_{max}}\left(1 - \left(\frac{r_{out}}{r_{in}}\right)^{1-f_0}\right)} \left(\frac{r_{in}}{r_{out}}\right)^{f_0} \tag{24}$$

Combining these equations, this means that the following overall model can be used:

$$\text{if } N_{Rf} > 1 : R_f = 1$$

$$\text{if } 1 > N_{Rf} > \frac{r_{in}}{r_{out}} : R_f = \frac{N_{Rf}}{\left(\frac{L_{in}}{L_{max}} + \left(1 - \frac{L_{in}}{L_{max}}\right){N_{Rf}}^{1-f_0}\right)}$$

$$\text{if } N_{Rf} < \frac{r_{in}}{r_{out}} : \tag{25}$$

$$R_f \geq \frac{N_{Rf}}{\left(\frac{L_{in}}{L_{max}} + \left(1 - \frac{L_{in}}{L_{max}}\right){N_{Rf}}^{1-f_0}\right)} \quad \text{and} \quad R_f \geq R_{f,min}$$

A pragmatic approach to the final condition could be to use the maximum of the two calculated froth recoveries (though noting that the model is not completely valid in this region):

$$\text{if } N_{Rf} < \frac{r_{in}}{r_{out}} : \tag{26}$$

$$R_f = max\left(\frac{N_{Rf}}{\left(\frac{L_{in}}{L_{max}} + \left(1 - \frac{L_{in}}{L_{max}}\right){N_{Rf}}^{1-f_0}\right)}, R_{f,min}\right)$$

Since N_{Rf} is high for very stable froths and/or very small particles, the froth recovery will approach 1 and therefore lose its dependency on either particle size or froth stability for any further increases in the value of N_{Rf}. Over intermediate values of N_{Rf} (i.e., $1 > N_{Rf} > \frac{r_{in}}{r_{out}}$), the froth recovery will be very strongly dependent on both the particle size and the froth stability. At low values of N_{Rf} (i.e. $N_{Rf} < \frac{r_{in}}{r_{out}}$), the dependency of the froth recovery on the froth stability will remain strong, but the dependency on particle size will become far less strong and eventually vanish. This is because, over these values of N_{Rf}, the number of particles that become detached will still strongly depend on stability, but virtually all of those that become detached will fall out of the froth irrespective of their size.

6. Froth recovery behaviour with a variable detachment fraction

If we assume that we are within the region of validity for the model and keep f_0 constant at a value of 0.05 and change the other two parameters in the model, namely N_{Rf} and L_{in}/L_{max}, we can obtain the froth recovery as a function of these two parameters (see Fig. 2). Given the ranges of validity discussed above and the fact that typical average bubble sizes in a flotation pulp will be of the order of a fraction of a millimetre to a few millimetres, while the overflowing bubble size will be within the range of a few millimetres up to possibly 10 cm or so, there will be a valid range for N_{Rf} covering about 3 orders of magnitude down from 1, though with a two order of magnitude or smaller change in bubble radius being more common.

N_{Rf} will be a function of 3 effects, namely particle size, froth stability and solids content in the Plateau borders. Both the particle size and the solids content will affect the particle settling velocity, while the froth stability will influence both the air recovery and the ratio of the incoming to outgoing bubble size.

$$N_{Rf} = \sqrt{\frac{v_g max(\alpha(1-\alpha), 0.25)}{v_{set}}}\left(\frac{r_{in}}{r_{out}}\right) \approx \frac{g(\text{solids content})h(\text{froth stability})}{d_{particle}} \tag{27}$$

Where $d_{particle}$ is the diameter of the particle being considered, $g(solidscontent)$ is an increasing function of solids content as settling velocity decreases with increasing solids content and $h(frothstability)$ is an increasing function of froth stability as both the air recovery and the ratio of the incoming to outgoing bubble size increase with increasing froth stability.

Since N_{Rf} is approximately inversely proportional to the particle diameter, it is also useful to plot the froth recovery versus the inverse of N_{Rf} as this will be proportional to the diameter of the particle being

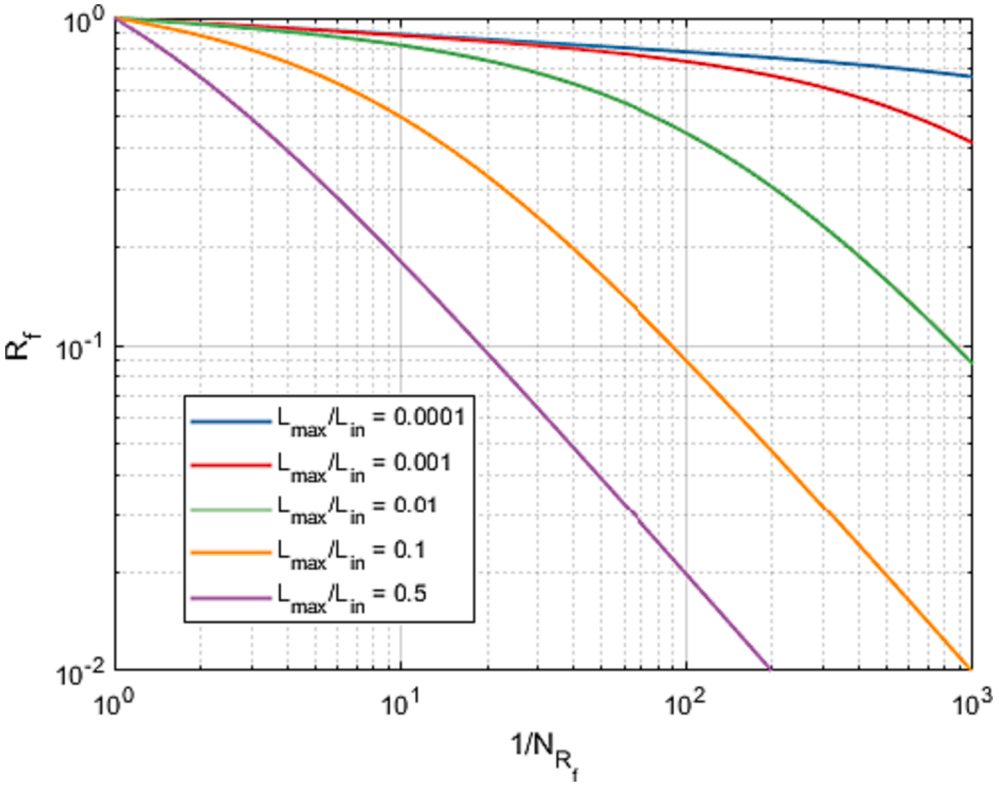


Fig. 3. Froth recovery as a function of the inverse of N_{Rf} for different ratios of the initial to maximum bubble loading.

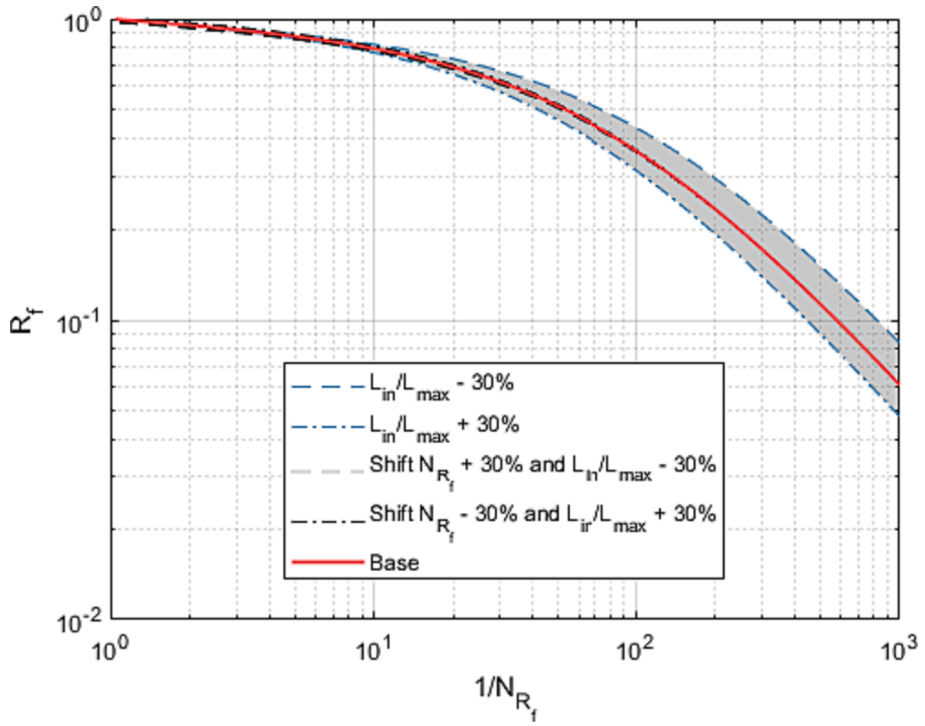


Fig. 4. Demonstrating the rough equivalence between changes in L_{in}/L_{max} and shifts in N_{Rf} for low values of L_{in}/L_{max} and f_0

considered, with a pre-factor that is dependent on the froth behaviour (i.e. feed and operating conditions), but constant for all the different particle sizes in a given cell. Fig. 3 shows the froth recovery as a function of the inverse of N_{Rf}.

If we consider what would be expected to happen down the bank for a set of flotation cells, there are two competing effects. Firstly, the froth stability and solids content within the Plateau borders will decrease down a bank of cells. These will both have the effect of decreasing N_{Rf} independently of the particle size effect (moving to the left in Fig. 2 and right in Fig. 3). This effect would tend to decrease the froth recovery for

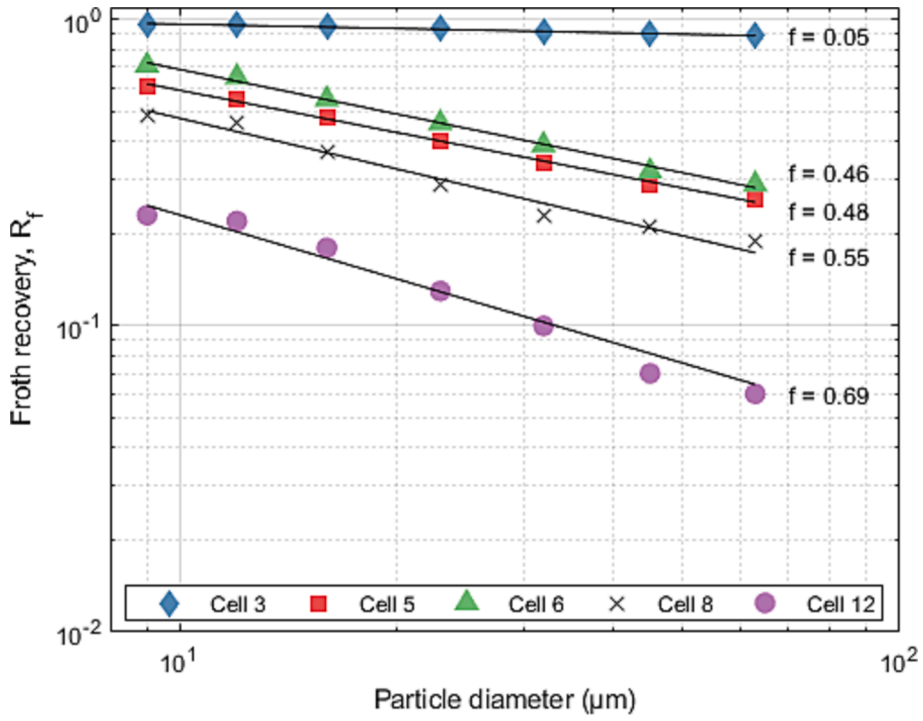


Fig. 5. Froth recovery vs particle size for cells down a bank (based on Savassi, 1998).

a given particle size as you move down a bank of cells. Physically this is caused by two effects, namely an increase in the amount of coalescence causing more particles to potentially fall off the bubble surfaces and a decrease in the water recovery, which will reduce the probability of previously attached particles being recovered to the concentrate unattached.

The other effect will be the impact of pulp zone loading on the behaviour. The pulp zone loading will decrease down a bank of cells. This will have the opposite impact to the froth stability and will tend to increase the froth recovery for a given particle size down a bank of cells. This is because low initial loading means that there is more free space on the bubbles and therefore a smaller fraction of them will become detached during a coalescence event. Since the recovery over a single cell will be highest at the beginning of the rougher bank, the change in loading will also be most pronounced at the beginning of a bank. This means that this effect may dominate over the first few cells, especially if

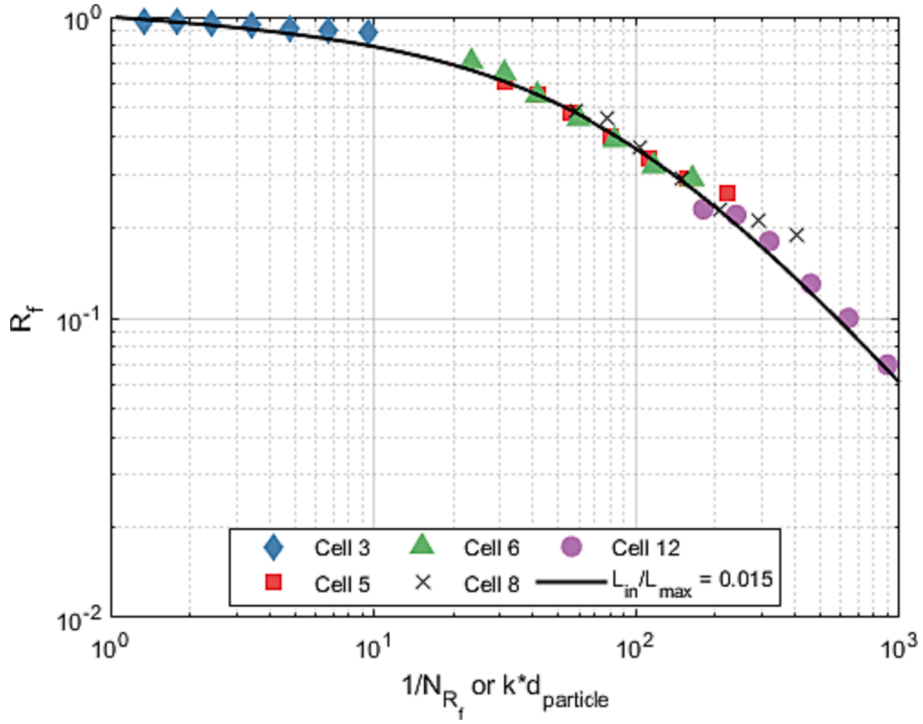


Fig. 6. Multiplying the particle sizes by a constant froth effect for each cell so that the experimental data forms a single curve.

Table 1
Multipliers required to align the data to the model. k is the factor by which the particle size needs to be scaled to adjust the froth recoveries onto the R_f vs $1/N_{Rf}$ curve (Fig. 6), while C is factor from equation (29) used to fit the model to the R_f vs particle size (Fig. 7). Note that k times C should be approximately the inverse of the loading ratio used when generating Fig. 6, though differences in fitting on log–log vs linear axes and the differences between the full (equation (20) and approximate (equation (28) mean that there is a small increase in this product down the bank.

Cell Number	k (microns^{-1}) – Fig. 6	C (microns) – Fig. 7
3	0.15	330.
5	2.6	19.6
6	3.5	15.3
8	6.5	9.39
12	20.0	3.44

the cells are close to being carrying capacity limited (Finch and Tan (2023); Neethling et al. (2019); Yianatos and Vallejos (2022)).

On log–log axes the loading ratio influences the position of the curve more strongly than it does the shape as long the initial loading ratio is much less than 1 (i.e., if the flotation cell is not close to being carrying capacity limited in the pulp). In other words, an increase in the loading ratio is roughly equivalent to multiplying N_{Rf} by a constant as long as the initial loading is much less than the maximum loading (see Fig. 4). The relative change required in N_{Rf} is also essentially the same as that in the loading to keep the curve the same. This is readily seen from equation (20), where if $f_0 \ll 1$ and $L_{in}/L_{max} \ll 1$ then:

$$R_f \approx N_{Rf}\frac{L_{max}}{L_{in}}\frac{1}{\left(1+N_{Rf}\frac{L_{max}}{L_{in}}\right)} \tag{28}$$

7. Experimental comparison

This model can be validated by examining size by size froth recoveries and how they vary down a bank of cells. One set of data that contains this information is that of (Savassi, 1998). In Fig. 4 this data is used to obtain the apparent value of f for cells at different locations down a bank. The f here is the average slope of the data on log–log axes and is thus the apparent value, which we would expect to see change with operating and feed conditions according to this new model.

From Fig. 5 it seems that for this plant there is a general trend for the froth recovery to drop and the apparent value of detachment probability to increase down the bank. This is consistent with the drop in stability (and potentially also the decrease in solids content in the Plateau borders) down the bank being the dominant effect rather than the loading change.

If we assume that the loading effect is small, we can estimate the relative change in the stability by multiplying the particle sizes for each of the separate curves so that then form a continuous curve. The multiplier for the first curve was set by knowing that the froth recovery should trend towards 1 as $1/N_{Rf}$ decreases towards 1. The resultant curve then fitted the model for a value of $L_{in}/L_{max} = 0.015$ quite well (see Fig. 6). Note that this value for the ratio is dependent on the exact multipliers used, though the basic shape of the curve is not strongly dependent on the exact value of the loading ratio as long as it is significantly less than one (see Fig. 4).

The multipliers, k, required to align the data to the theory for a constant value of the initial loading are as shown in Table 1..

Since the fitting in Fig. 6 corresponds to a low L_{in}/L_{max} ratio and the experimental data suggests that f_0 is also low, it is appropriate to use equation (28) to model this data. Note that the assumption that the incoming bubble surface loading is much lower than the maximum bubble surface loading is not always appropriate, especially in the first cells in some rougher banks or in some cleaner banks, which can both potentially be carrying capacity limited. Since settling velocity is approximately proportional to the square of the particle diameter, for a given flotation cell we can say that

$$N_{Rf}\frac{L_{max}}{L_{in}} \approx \frac{C}{d_{particle}} \tag{29}$$

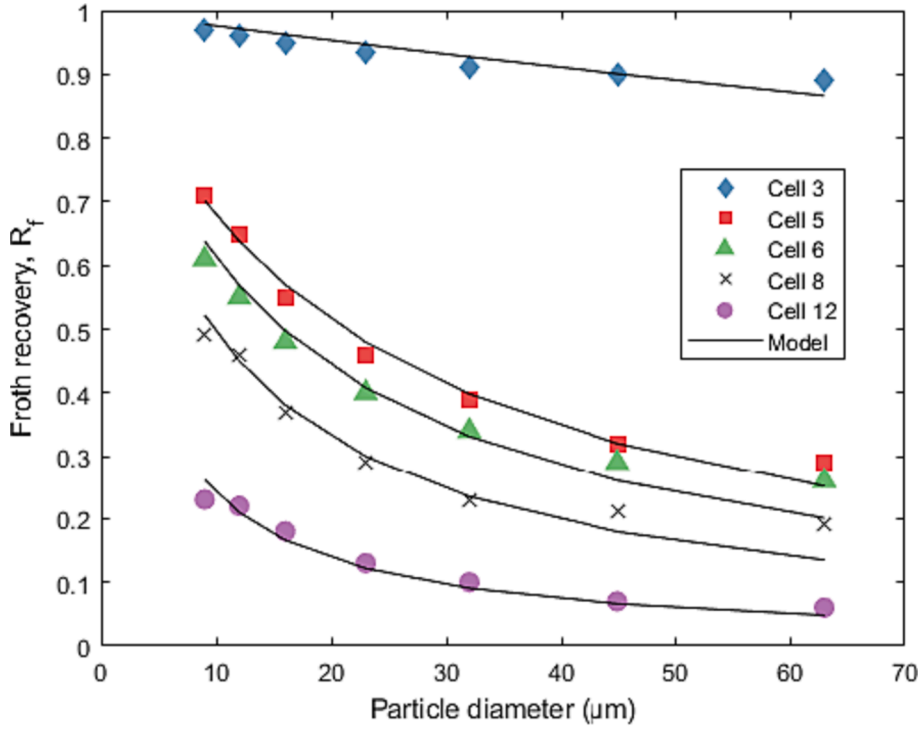


Fig. 7. Experimental vs model froth recovery as function of particle size for different cells down a bank using a single fitting parameter based on equation (28) (experimental data based on Savassi, 1998).

Where C is characteristic of the performance of a given cell, increasing with froth stability and decreasing with the ratio of incoming to maximum bubble surface loading. It thus allows the particle size effect to be separated from the other influences on froth recovery (assuming that there is not a strong relationship between particle size and particle density). In Fig. 7 equation (28) and (29) are used to model the froth recovery behaviour, where the value of C forms a single fitting parameter for each of the cell's relationship between froth recovery and particle size. C is also a characteristic particle size and, at least when using the simplified model represented by equation (28), is equal to the particle size at which the froth recovery is 0.5. It can be seen that the shape of this relationship is quite accurately captured, including how it changes with position down the bank and, thus also, froth stability based on only a single fitting parameter for each cell.

8. Conclusions

In this paper, we have introduced an improved model for froth recovery. The key difference to the previous model developed by the authors is the inclusion of a detachment probability that depends on the bubble loading. This inclusion results in a phenomenological model in which the froth recovery depends on two dimensionless groups. The first group depends on particle settling velocity, which in turn is determined by particle density and size, the superficial air velocity within the froth, and two froth stability parameters: the change in bubble size over the froth and air recovery. The second dimensionless group is the ratio of the surface loading of the bubbles entering the froth to the maximum possible surface loading.

Our findings showed that at low relative loadings, these two dependencies can be combined into a single dependency, as illustrated in equations (28) and (29). However, at high incoming loadings, i.e., when the cell is close to its carrying capacity limit, the dependencies operate independently of each other. In these situations, the more complete model represented by equation (20) needs to be used. In both cases it is important to be cautious around the ranges of validity of the modelling, as represented by equations (25) and (26).

This improved model allows the evolution of the froth recovery to be explained, both with respect to particle size and down a bank of cells, as validated with measurements from an industrial flotation bank. This new model paves the way for a more accurate and insightful understanding of froth recovery and its dependency on both froth stability and particle properties.

CRediT authorship contribution statement

S.J. Neethling: Conceptualization, Methodology, Writing – original draft. **D. Mesa:** Investigation, Formal analysis, Visualization, Writing – review & editing. **P.R. Brito-Parada:** Investigation, Formal analysis, Writing – review & editing.

Declaration of Competing Interest

The authors declare the following financial interests/personal relationships which may be considered as potential competing interests: [Editor of Minerals Engineering - Pablo Brito-Parada].

Data availability

Data will be made available on request.

References

Finch, J.A., Dobby, G.S., 1990. Column flotation. Pergamon Press ISBN 13, 9780080401867.

Finch, J.A., Tan, Y.H., 2023. On limits to flotation cell size. Minerals 13 (3), 411. https://doi.org/10.3390/MIN13030411.

Hadler, K., 2015. The link between froth surface grade and flotation feed grade. Miner. Eng. 78, 32–37. https://doi.org/10.1016/J.MINENG.2015.03.024.

Neethling, S.J., 2008. Simple approximations for estimating froth recovery. Int. J. Miner. Process. 89 (1–4) https://doi.org/10.1016/j.minpro.2008.09.007.

Neethling, S.J., Cilliers, J.J., 2003. Modelling flotation froths. Int. J. Miner. Process. 72 (1–4) https://doi.org/10.1016/S0301-7516(03)00104-2.

Neethling, S.J., Cilliers, J.J., 2009. The entrainment factor in froth flotation: Model for particle size and other operating parameter effects. Int. J. Miner. Process. 93 (2) https://doi.org/10.1016/j.minpro.2009.07.004.

Neethling, S.J., Cilliers, J.J., Woodburn, E.T., 2000. Prediction of the water distribution in a flowing foam. Chem. Eng. Sci. 55 (19) https://doi.org/10.1016/S0009-2509(00)00054-3.

Neethling, S.J., Cilliers, J.J., 2002a. Solids motion in flowing froths. Chem. Eng. Sci. 57 (4) https://doi.org/10.1016/S0009-2509(01)00393-1.

Neethling, S.J., Cilliers, J.J., 2002b. The entrainment of gangue into a flotation froth. Int. J. Miner. Process. 64 (2–3) https://doi.org/10.1016/S0301-7516(01)00067-9.

Neethling, S.J., Lee, H.T., Cilliers, J.J., 2003. Simple relationships for predicting the recovery of liquid from flowing foams and froths. Miner. Eng. 16 (11) https://doi.org/10.1016/j.mineng.2003.06.014.

Neethling, S.J., Lee, H.T., Grassia, P., 2005. The growth, drainage and breakdown of foams. Colloids Surf A Physicochem Eng Asp 263 (1–3 SPEC. ISS). https://doi.org/10.1016/j.colsurfa.2004.12.014.

Neethling, S.J., Brito-Parada, P.R., Hadler, K., Cilliers, J.J., 2019. The transition from first to zero order flotation kinetics and its implications for the efficiency of large flotation cells. Miner. Eng. 132, 149–161. https://doi.org/10.1016/j.mineng.2018.11.039.

Rahman, R.M., Ata, S., Jameson, G.J., 2012. The effect of flotation variables on the recovery of different particle size fractions in the froth and the pulp. Int. J. Miner. Process. 106–109, 70–77. https://doi.org/10.1016/J.MINPRO.2012.03.001.

Sadr-Kazemi, N., Cilliers, J.J., 1997. An image processing algorithm for measurement of flotation froth bubble size and shape distributions. Miner. Eng. 10 (10) https://doi.org/10.1016/s0892-6875(97)00094-0.

Sadr-Kazemi, N., Cilliers, J.J., 2000. Technique for measuring flotation bubble shell thickness and concentration. Miner. Eng. 13 (7) https://doi.org/10.1016/S0892-6875(00)00061-3.

Savassi, O.N., 1998. Direct estimation of the degree of entrainment and the froth recovery of attached particles in industrial flotation cells. Julius Krutschnitt Mineral Research Centre, PhD.

Ventura-Medina, E., Barbian, N., Cilliers, J.J., 2004. Solids loading and grade on mineral froth bubble lamellae. Int. J. Miner. Process. 74 (1–4) https://doi.org/10.1016/j.minpro.2003.11.001.

Yianatos, J.B., Moys, M.H., Contreras, F., Villanueva, A., 2008. Froth recovery of industrial flotation cells. Miner. Eng. 21 (12–14), 817–825. https://doi.org/10.1016/J.MINENG.2007.12.012.

Yianatos, J., Vallejos, P., 2022. Limiting conditions in large flotation cells: Froth recovery and bubble loading. Miner. Eng. 185, 107695. https://doi.org/10.1016/J.MINENG.2022.107695.